

Two energy scales in the spin excitations of the high- T_c superconductor $\text{La}_{2-x}\text{Sr}_x\text{CuO}_4$

B. Vignolle,¹ S.M. Hayden,¹ D.F. McMorrow,^{2,3} H.M. Rønnow,⁴ B. Lake,⁵ C.D. Frost,³ and T.G. Perring³

¹*H.H. Wills Physics Laboratory, University of Bristol, Tyndall Ave., Bristol, BS8 1TL, UK*

²*London Centre for Nanotechnology and Department of Physics and Astronomy,
University College London, London, WC1E 6BT, UK*

³*ISIS Facility, Rutherford Appleton Laboratory, Chilton, Didcot, Oxfordshire OX11 0QX, UK*

⁴*Laboratory for Neutron Scattering, ETH-Zürich and Paul Scherrer Institut, 5232 Villigen, Switzerland*

⁵*Hahn-Meitner Institut, Berlin D-14109, Germany.*

The excitations responsible for producing high-temperature superconductivity in the cuprates have not been identified. Two promising candidates are collective spin excitations and phonons [1]. A recent argument against spin excitations has been their inability to explain structures seen in electronic spectroscopies such as photoemission [2, 3, 4, 5] and tunnelling [6]. Here we use inelastic neutron scattering to demonstrate that collective spin excitations in optimally doped $\text{La}_{2-x}\text{Sr}_x\text{CuO}_4$ are more structured than previously thought. The excitations have a two component structure with a low-frequency component strongest around 18 meV and a broader component strongest near 40-70 meV. The second component carries most of the spectral weight and its energy matches structure seen in photoemission and tunnelling spectra [2, 3, 4, 5, 6] in the range 50-90 meV. Our results demonstrate that collective spin excitations can explain features of quasiparticle spectroscopies and are therefore likely to be the strongest coupled excitations.

Since their discovery, considerable progress has been made in understanding the properties of the high- T_c cuprate superconductors. For example, we know that the superconductivity involves Cooper pairs, as in the conventional BCS theory, but the d -wave pairing is different to the s -wave pairing of conventional superconductors. However, a major outstanding issue is the pairing mechanism. Identifying the bosonic excitations which were strongly coupled to the electron quasiparticles played an pivotal role in confirming the pairing mechanism in conventional superconductors [7, 8]. In the case of the copper oxide superconductors, advances in electronic spectroscopies such as angle resolved photoemission (ARPES) and tunnelling have revealed structure in the low-energy electronic excitations which may reflect coupling to bosonic excitations. ARPES measurements on $\text{Bi}_2\text{Sr}_2\text{CaCu}_2\text{O}_8$, $\text{Bi}_2\text{Sr}_2\text{CuO}_6$ and $\text{La}_{2-x}\text{Sr}_x\text{CuO}_4$ have shown that there are rapid changes or “kinks” in the quasiparticle dispersion $E(k)$ in the nodal direction [$\mathbf{k} \parallel (1/2, 1/2)$] for energies in the range 50–80 meV [2, 3, 4, 5]. The origin of these kinks has been discussed in terms of coupling to collective spin excitations and phonons. Optical conductivity measurements also

suggest that there are strongly coupled electronic excitations in this energy range [9]. Unfortunately, the high-energy magnetic excitations in the cuprates have been most comprehensively studied in $\text{YBa}_2\text{Cu}_3\text{O}_{6+x}$, a compound for which ARPES data are scarce. In contrast, $\text{La}_{2-x}\text{Sr}_x\text{CuO}_4$ is a system for which the magnetic excitations may be studied by neutron scattering (because of the availability of large single crystals) and ARPES (because a suitable surface may be prepared).

Here we report a high-resolution neutron scattering study of the magnetic excitations in optimally doped $\text{La}_{2-x}\text{Sr}_x\text{CuO}_4$ ($x=0.16$, $T_c=38.5$ K). The parent compound La_2CuO_4 of the $\text{La}_{2-x}\text{Sr}_x\text{CuO}_4$ superconducting series exhibits antiferromagnetic order with an ordering wavevector of $\mathbf{Q}_{2D}=(1/2, 1/2)$. Doping induces superconductivity and causes low-frequency incommensurate fluctuations [10, 11] to develop with wavevectors $\mathbf{Q}_{2D} = (1/2, 1/2 \pm \delta)$ and $(1/2 \pm \delta, 1/2)$. These excitations broaden [12] and disperse inwards initially towards $(1/2, 1/2)$ [13] with increasing energy. The present work extends the energy range and wavevector resolution of previous studies [10, 11, 12, 13, 14].

Neutron spectroscopy provides a direct probe of the magnetic response function $\chi''(\mathbf{Q}, \omega)$. Experiments were performed on the MAPS spectrometer at the ISIS spallation neutron source of the Rutherford-Appleton Laboratory. Figure 1a-h shows wavevector-dependent images of the magnetic response at various energies demonstrating how it evolves with energy. At low energies, $E = 10$ meV (panel 1a) we observe the low-energy incommensurate excitations [10, 11, 12, 13]. As the energy is increased, $E = 18$ meV (panel 1b) the response becomes stronger, the pattern fills in along the line connecting the nearest neighbour incommensurate peaks and the incommensurability δ decreases. For $E = 25$ meV (panel 1c), the intensity of the pattern is noticeably attenuated. On further increasing to $E = 41$ meV (panel 1d), the response “recovers”, becoming more intense again, but is now peaked at the commensurate wavevector $(1/2, 1/2)$. At higher energy $E = 90$ meV (panel 1e), the structure resembles a square box with the corners pointing along the (110) type directions, *i.e.* towards the Brillouin zone center. Thus the square pattern is rotated 45° with respect to the low energy response (e.g. panel 1b). A similar high-energy response has been observed

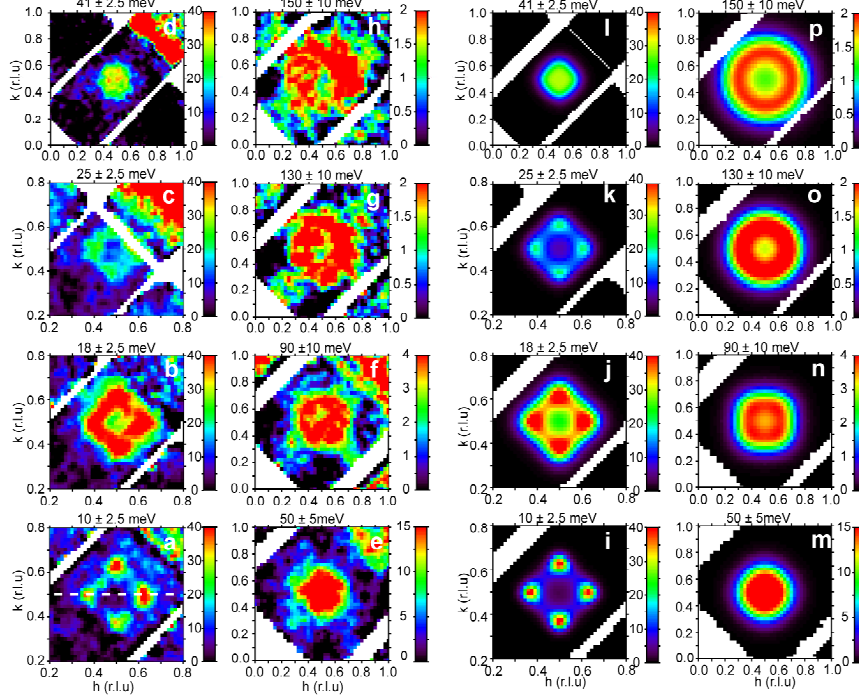


FIG. 1: **Images of the magnetic excitations in $\text{La}_{1.84}\text{Sr}_{0.16}\text{CuO}_4$ for various energies at $T=12$ K.** **a-h** The measured $\chi''(\mathbf{Q}, \omega)$ is plotted in units of $\mu_B^2 \text{ eV}^{-1} \text{ f.u.}^{-1}$ as a function of wavevector. **a-c** show the emergence and disappearance of the component at $(1/2 \pm \delta, 1/2)$ and $(1/2, 1/2 \pm \delta)$ which is most intense at lower energies. **d-h** show the higher energy component which emerges around 41 meV and disperses outwards with increasing energy. **i-p** Model fits to the images of the magnetic excitations shown in **a-h**. The phenomenological model [Eq. (1)] provides a good description of the experimentally measured magnetic excitations and can therefore be used to parameterize the data. At higher energies (panels **n-p**) the data are best fitted with the model $\chi''(\mathbf{Q}, \omega)$ rotated 45° in the $h - k$ plane. Wavevectors are labelled by their positions in reciprocal space $\mathbf{Q} = h\mathbf{a}^* + k\mathbf{b}^* + l\mathbf{c}^*$.

in underdoped $\text{YBa}_2\text{Cu}_3\text{O}_{6+x}$ [15, 16] and the stripe ordered composition $\text{La}_{1.875}\text{Ba}_{0.125}\text{CuO}_4$ [17]. Thus a rotated continuum appears to be a universal feature of the cuprates.

In order to make our analysis quantitative, we fitted a modified Lorentzian cross-section previously used to describe the cuprates and other systems [18] to the data:

$$\chi''(\mathbf{Q}, \omega) = \chi_\delta(\omega) \frac{\kappa^4(\omega)}{[\kappa^2(\omega) + R(\mathbf{Q})]^2} \quad (1)$$

with

$$R(\mathbf{Q}) = \frac{[(h - \frac{1}{2})^2 + (k - \frac{1}{2})^2 - \delta^2]^2 + \lambda(h - \frac{1}{2})^2(k - \frac{1}{2})^2}{4\delta^2}$$

where $\kappa(\omega)$ is an inverse correlation length, the position of the four peaks is specified by δ , and λ controls the shape of the pattern ($\lambda=4$ corresponds to four distinct peaks and $\lambda=0$ corresponds to a pattern with circular symmetry).

Fig. 1i-p shows plots of the fitted model response for the same energies as Fig. 1a-h. Another way of displaying the results is to take constant energy cuts through our data set. Fig. 2 shows cuts along the dashed trajectory in Fig. 1 for various energies together with fits of our model response (Eq. 1) convolved with the experimental resolution. The good agreement between the data and fits allows us to use the parameters derived from the fits

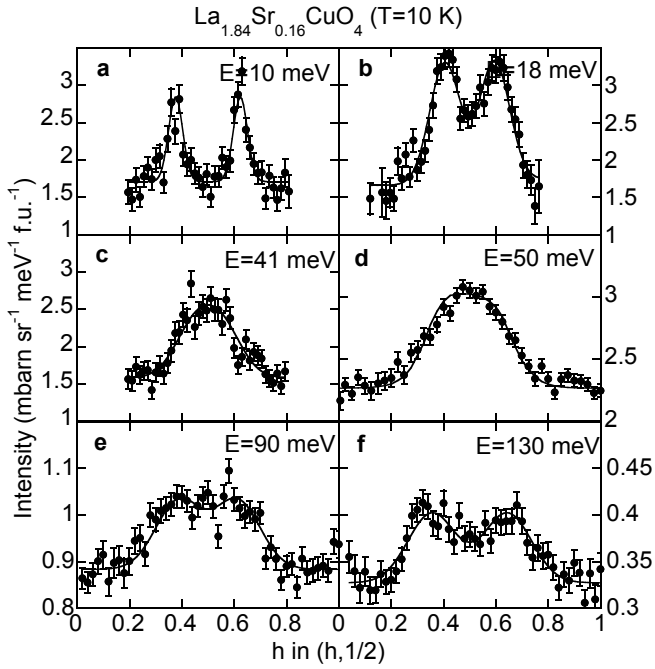


FIG. 2: **Magnetic excitations in $\text{La}_{1.84}\text{Sr}_{0.16}\text{CuO}_4$ at $T=12$ K.** **a-f** show the variation of the scattered intensity with wavevector for various fixed excitation energy. The trajectory of the cut is shown by the dashed line in Fig. 1a. **a-b** show the incommensurate low-frequency component of the response. The high-frequency component is strongest for 40–50 meV (**c-f**). Two distinct peaks are seen at higher energies (**e-f**), these disperse away from $(1/2, 1/2)$ in a similar manner to the spin-wave excitations in the parent compound La_2CuO_4 .

(Fig. 3) to interpret our results. In order to distinguish between magnetic and phonon scattering the experiment was performed at a number of incident energies. This means that the same in-plane momentum (h, k) could be probed with a variety of l (momentum perpendicular to plane) values and strong phonons isolated. The fact that data collected with different incident energies yields similar results confirms the validity of our analysis. We have expressed the strength of the spin fluctuations in terms of the local or wavevector-averaged susceptibility $\chi''(\omega) = \int \chi''(\mathbf{Q}, \omega) d^3Q / \int d^3Q$ determined from the fitted cross-section. The local susceptibility $\chi''(\omega)$ is a measure of the density of magnetic excitations for a given energy.

Figure 3a illustrates one of the key results of this work: the magnetic response of $\text{La}_{1.84}\text{Sr}_{0.16}\text{CuO}_4$ has a two component structure. The lower-energy peak corresponds to the incommensurate structure which is rapidly attenuated above 20 meV. The higher-energy structure is peaked at $(1/2, 1/2)$ for $E \approx 40$ –50 meV and broadens out with increasing energy above this. Although the wavevector-averaged susceptibility $\chi''(\omega)$ of the higher frequency component is peaked around 50 meV, it has a long tail with a measurable response at highest ener-

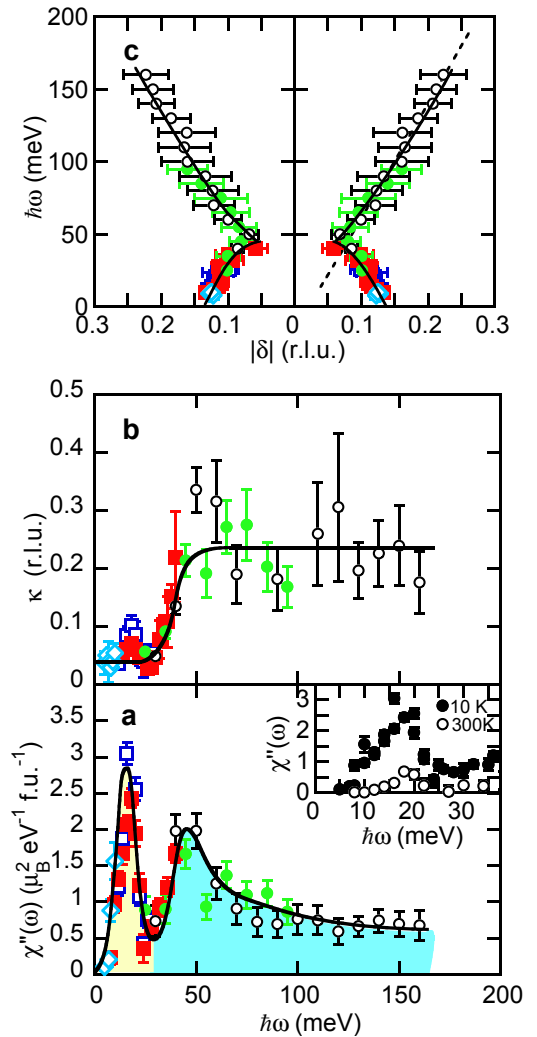


FIG. 3: **Magnetic excitation spectrum and evolution of the form of the magnetic response with energy.** The susceptibility wavevector-averaged susceptibility $\chi''(\omega)$ (**a**) shows a “peak-dip-hump” structure suggesting that the magnetic response has two components. The emergence of the higher frequency component above about 40 meV corresponds to a broadening of response in wavevector as demonstrated by the rapid increase in the κ (**b**). There is a strong dispersion of the peak positions in constant excitation-energy cuts as shown by the energy dependence of the incommensurability $\delta(\omega)$ (**c**). The high-energy dispersion indicates the persistence of residual antiferromagnetic interactions. Symbols indicate different incident energies: $E_i = 30(\diamond), 55(\square), 90(\blacksquare), 160(\bullet), 240$ meV (\circ).

gies probed ($E=155$ meV) in this experiment. The observed two component structure differs from the response observed in the magnetically ordered but weakly superconducting compound $\text{La}_{1.875}\text{Ba}_{0.125}\text{CuO}_4$ [17] which does not show the lower peak in $\chi''(\omega)$. Although $\text{La}_{1.875}\text{Ba}_{0.125}\text{CuO}_4$ does a similar dispersion in $|\delta|$.

Given the markedly different characteristics of the two components which make up the magnetic response in

$\text{La}_{1.84}\text{Sr}_{0.16}\text{CuO}_4$, it is likely that they have different origins. One possible scenario is that the lower-energy incommensurate structure is due to quasiparticle (electron-hole) pair creation which might be calculated from an underlying band structure [19, 20], while the higher-energy structure is due to the residual antiferromagnetic interactions. It is interesting to compare the magnetic response at optimal doping with that of the antiferromagnetic parent compound La_2CuO_4 [21]. In La_2CuO_4 , $\chi''(\omega)$ is approximately constant over the energy range probed here (0–160 meV) with $\chi''(\omega) \approx 1.7 \mu_B^2 \text{ eV}^{-1} \text{ f.u.}^{-1}$. Thus the effect of doping is to suppress the high-energy response ($\hbar\omega > 50$ meV) and enhance the response at lower frequencies, creating a double peak structure. Fig. 3c shows that the high energy part of the response disperses with increasing energy. Constant energy cuts through the data yield two peaks (see Fig. 2) which are reminiscent of spin wave in the parent compound La_2CuO_4 . We may use the high-energy dispersion to estimate an effective Heisenberg exchange constant J which quantifies the strength of the coupling between the copper spins. Using the fitted values of $|\delta|$ in Fig. 3c for $E > 40$ meV, we estimate the gradient to be $dE/d\delta = 510 \pm 50 \text{ meV}\text{\AA}^{-1}$. This may then be compared with the standard expression for the spin wave velocity in a square lattice antiferromagnet, $\hbar v_s = Z_c \sqrt{8S}Ja$, where Z_c , S , and a are the quantum renormalization, spin, and lattice parameter respectively. We find that the effective exchange constant for $\text{La}_{1.84}\text{Sr}_{0.16}\text{CuO}_4$ is $J = 81 \pm 9$ meV. This is substantially reduced from the parent compound La_2CuO_4 where $J = 146 \pm 4$ meV [21].

It is interesting to compare our measurements with electronic spectroscopy performed on cuprate superconductors with the same energy scale. The energy of the 50 meV peak matches the energy range (40–70 meV) where angle resolved photoemission spectroscopy (ARPES) measurements [5] in the same compound $\text{La}_{2-x}\text{Sr}_x\text{CuO}_4$ show rapid changes or kinks in the quasiparticle dispersion $E(k)$. These kinks may well be caused by coupling to the spin excitations reported here. At higher energies, ARPES measurements suggest that the quasiparticles are coupled to bosonic excitations with energies up to at least 300 meV [22]. This would match the tail of the collective spin excitations which we observe here (Fig. 3a). Other electronic spectroscopy data is not available $\text{La}_{2-x}\text{Sr}_x\text{CuO}_4$. However, we may compare with other systems. Infrared conductivity measurements provide evidence of coupling to high energy excitations in, for example, $\text{YBa}_2\text{Cu}_3\text{O}_{6+x}$ [23] and $\text{Bi}_2\text{Sr}_2\text{Ca}_{0.92}\text{Y}_{0.08}\text{Cu}_2\text{O}_{8+\delta}$ [24]. In addition tunnelling measurements on $\text{Bi}_2\text{Sr}_2\text{CaCu}_2\text{O}_{8+\delta}$ [25] show evidence of coupling to a sharp mode near 40 meV and broader excitations extending above 100 meV.

In summary, we use neutron scattering measurements to show that the collective magnetic excitations in optimally doped $\text{La}_{2-x}\text{Sr}_x\text{CuO}_4$ are made up of two com-

ponents. At low energies, the excitations are incommensurate and disperse with increasing energy towards the commensurate antiferromagnetic ordering wavevector of La_2CuO_4 , peaking in intensity around 20 meV. At higher energies a second component develops which displays a broad, commensurate peak around 50 meV. It then displays a spin-wave-like dispersion at higher energies. The high-frequency excitations are most naturally interpreted as being due to residual antiferromagnetic interactions. Comparison of the present data with electron photoemission and tunnelling data suggests that it is this high-frequency component which affects the electron quasiparticles most strongly. As the excitations that couple most effectively to the quasiparticles are most likely to play an important part in the superconducting pairing, our results support the notion that high- T_c superconductivity is magnetically mediated.

- [1] Chubukov, A. V., Pines, D. & Schmalian, J. A spin fluctuation model for d -wave superconductivity. In K. H. Bennemann & J. B. Ketterson, eds., *The Physics of Superconductors*, vol. 2, pp. 495–590 (Springer, Berlin, 2003).
- [2] Bogdanov, P. V. *et al.* Evidence for an energy scale for quasiparticle dispersion in $\text{Bi}_2\text{Sr}_2\text{CaCu}_2\text{O}_8$. *Phys. Rev. Lett.* **85**, 2581–2584 (2000).
- [3] Kaminski, A. *et al.* Renormalization of spectral line shape and dispersion below T_c in $\text{Bi}_2\text{Sr}_2\text{CaCu}_2\text{O}_{8+\delta}$. *Phys. Rev. Lett.* **86**, 1070–1073 (2001).
- [4] Johnson, P. D. *et al.* Doping and temperature dependence of the mass enhancement observed in the cuprate $\text{Bi}_2\text{Sr}_2\text{CaCu}_2\text{O}_{8+\delta}$. *Phys. Rev. Lett.* **87**, 177007 (2001).
- [5] Lanzara, A. *et al.* Evidence for ubiquitous strong electron-phonon coupling in high-temperature superconductors. *Nature* **412**, 510–514 (2001).
- [6] Lee, J. *et al.* Interplay of electron-lattice interactions and superconductivity in $\text{Bi}_2\text{Sr}_2\text{CaCu}_2\text{O}_{8+\delta}$. *Nature* **442**, 546–550 (2006).
- [7] McMillan, W. L. & Rowell, J. M. Lead phonon spectrum calculated from superconducting density of states. *Phys. Rev. Lett.* **14**, 108–112 (1965).
- [8] Stedman, R., Almqvist, L. & Nilsson, G. Phonon-frequency distributions and heat capacities of aluminum and lead. *Phys. Rev.* **162**, 549–557 (1967).
- [9] Basov, D. N. & Timusk, T. Electrodynamics of high- T_c superconductors. *Rev. Mod. Phys.* **77**, 721–779 (2005).
- [10] Shirane, G. *et al.* Temperature dependence of the magnetic excitations in $\text{La}_{1.85}\text{Sr}_{0.15}\text{CuO}_4$ ($T_c = 33\text{K}$). *Phys. Rev. Lett.* **63**, 330–333 (1989).
- [11] Cheong, S. W. *et al.* Incommensurate magnetic fluctuations in $\text{La}_{2-x}\text{Sr}_x\text{CuO}_4$. *Phys. Rev. Lett.* **67**, 1791–1794 (1991).
- [12] Mason, T. E., Aeppli, G. & Mook, H. A. Magnetic dynamics of superconducting $\text{La}_{1.86}\text{Sr}_{0.14}\text{CuO}_4$. *Phys. Rev. Lett.* **68**, 1414–1417 (1992).
- [13] Christensen, N. B. *et al.* Dispersive excitations in the high-temperature superconductor $\text{La}_{2-x}\text{Sr}_x\text{CuO}_4$. *Phys. Rev. Lett.* **93**, 147002 (2004).

[14] Hayden, S. M. *et al.* Comparison of the high-frequency magnetic fluctuations in insulating and superconducting $\text{La}_{2-x}\text{Sr}_x\text{CuO}_4$. *Phys. Rev. Lett.* **76**, 1344–1347 (1996).

[15] Hayden, S. M., Mook, H. A., Dai, P. C., Perring, T. G. & Dogan, F. The structure of the high-energy spin excitations in a high-transition-temperature superconductor. *Nature* **429**, 531–534 (2004).

[16] Stock, C. *et al.* From incommensurate to dispersive spin-fluctuations: The high-energy inelastic spectrum in superconducting $\text{YBa}_2\text{Cu}_3\text{O}_{6.5}$. *Phys. Rev. B* **71**, 024522 (2005).

[17] Tranquada, J. M. *et al.* Quantum magnetic excitations from stripes in copper oxide superconductors. *Nature* **429**, 534–538 (2004).

[18] Sato, H. & Maki, K. Theory of inelastic neutron scattering from Cr and its alloys near the Néel temperature. *Int. J. Magn.* **6**, 183–209 (1974).

[19] Si, Q. M., Zha, Y. Y., Levin, K. & Lu, J. P. Comparison of spin dynamics in $\text{YBa}_2\text{Cu}_3\text{O}_{7-\delta}$ and $\text{La}_{2-x}\text{Sr}_x\text{CuO}_4$ - effects of fermi-surface geometry. *Phys. Rev. B* **47**, 9055–9076 (1993).

[20] Littlewood, P. B., Zaanen, J., Aeppli, G. & Monien, H. Spin fluctuations in a 2-dimensional marginal fermi-liquid. *Phys. Rev. B* **48**, 487–498 (1993).

[21] Coldea, R. *et al.* Spin waves and electronic interactions in La_2CuO_4 . *Phys. Rev. Lett.* **86**, 5377–5380 (2001).

[22] Kordyuk, A. A. *et al.* Constituents of the quasiparticle spectrum along the nodal direction of high- T_c cuprates. *Phys. Rev. Lett.* **97**, 017002 (2006).

[23] Basov, D. N. *et al.* Pseudogap and charge dynamics in CuO_2 planes in ybco. *Phys. Rev. Lett.* **77**, 4090–4093 (1996).

[24] van der Marel, D. *et al.* Quantum critical behaviour in a high- T_c superconductor. *Nature* **425**, 271–274 (2003).

[25] Zasadzinski, J. F. *et al.* Persistence of strong electron coupling to a narrow boson spectrum in overdoped $\text{Bi}_2\text{Sr}_2\text{CaCu}_2\text{O}_{8+\delta}$ tunneling data. *Phys. Rev. Lett.* **96**, 017004 (2006).